Bioorganic & Medicinal Chemistry 16 (2008) 8287–8293

Contents lists available at ScienceDirect

Bioorganic & Medicinal Chemistry

journal homepage: www.elsevier.com/locate/bmc

Hybridization-dependent fluorescence of oligodeoxynucleotides incorporating new pyrene-modified adenosine residues

Kohji Seio, Masanhiro Mizuta, Kaori Tasaki, Keigo Tamaki, Akihiro Ohkubo, Mitsuo Sekine *

Department of Life Science, Tokyo Institute of Technology and CREST, JST Nagatsuda, Midoriku, Yokohama 226-8501, Japan

ARTICLE INFO

Article history:
Received 22 February 2008
Revised 16 May 2008
Accepted 16 May 2008
Available online 22 May 2008

Keywords:
Pyrene
Fluorescence
ODN
Size discrimination

ABSTRACT

We report the synthesis and properties of oligonucleotides incorporating N^6-[*N*-(pyren-1-ylmethyl)carbamoyl]-deoxyadenosine (dA^{pymcm}). We designed the ODN which incorporated two consecutive dA^{pymcm} residues. It was revealed that on hybridization with the target DNA and RNA oligomers, the fluorescence spectra of ODNs having two consecutive dA^{pymcm} molecules near the 5′-terminal position can change from the pyrene monomer emission to the excimer, depending on the chain length of the target DNA and RNA. These results indicated that dA^{pymcm}-modified ODNs can be used as interesting hybridization sensors that are sensitive to the size of the target strand.

1. Introduction

Fluorescent oligodeoxynucleotides (ODNs) with pyrene residues have been widely used as molecular probes for the hybridization and structure modification of functional nucleic acids.[1–13] Pyrene modifications have attracted attention because of the chemical stability and large solvatochromic effect of pyrene residues.[1–5,14] Moreover, two pyrene residues introduced in close proximity to each other can form a pyrene excimer that has a unique fluorescence absorbance around 480 nm.[6–13]

For example, Okamoto et al. reported purine and pyrimidine nucleoside derivatives having a pyrene residue at position 5 of pyrimidine bases, and demonstrated their photochemical base discrimination.[5] In addition, Yamana and co-workers reported oligonucleotides incorporating a uridine residue having a pyrenylmethyl group at the 2′-hydroxyl group and developed an RNA-selective hybridization sensor[4] and dipyrenyl-labeled ODNs for SNPs analysis.[8] Apart from such modifications at the sugar moiety and aromatic rings of nucleobases, we have researched the functionalization of the amino group of nucleosides[15] because a functional group at the amino groups can interact with complementary strands or their upstream and downstream bases through stacking interactions.[15,16] In this study, we report the preparation of a deoxyadenosine derivative (dA^{pymcm}) having a pyrenylmethylcarbamoyl group attached to the amino group (Fig. 1), and the synthesis and properties of ODNs incorporating this modified deoxynucleoside.

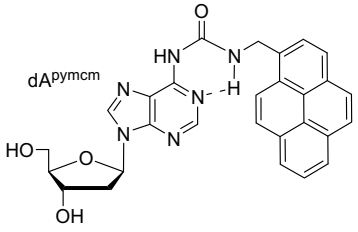

Figure 1. Structure of dA^{pymcm}.

These modified ODNs showed interesting fluorescence properties upon hybridization with complementary DNA or RNA strands. Moreover, it was revealed that on hybridization with the target DNA and RNA oligomers, the fluorescence spectra of ODNs having two consecutive dA^{pymcm} molecules near the 5′-terminal position can change the ratio of the pyrene monomer's emission at around 400 nm and the excimer's at around 480 nm, depending on the chain length of the target DNA and RNA. These results indicated that dA^{pymcm}-modified ODNs can be used as interesting hybridization sensors that are sensitive to the size of the target strand.

2. Results and discussion

2.1. Synthesis of oligodeoxynucleotides incorporating dA^{pymcm}

The phosphoramidite unit of dA^{pymcm} (**3**) was synthesized as shown in Scheme 1. Pyrenylmethylamine hydrochloride was coupled with 1.2 equiv of 4-nitrophenyl chloroformate in the presence

* Corresponding author. Tel.: +81 45 924 5706; fax: +81 45 924 5772.
E-mail address: msekine@bio.titech.ac.jp (M. Sekine).

0968-0896/$ - see front matter © 2008 Elsevier Ltd. All rights reserved.
doi:10.1016/j.bmc.2008.05.042

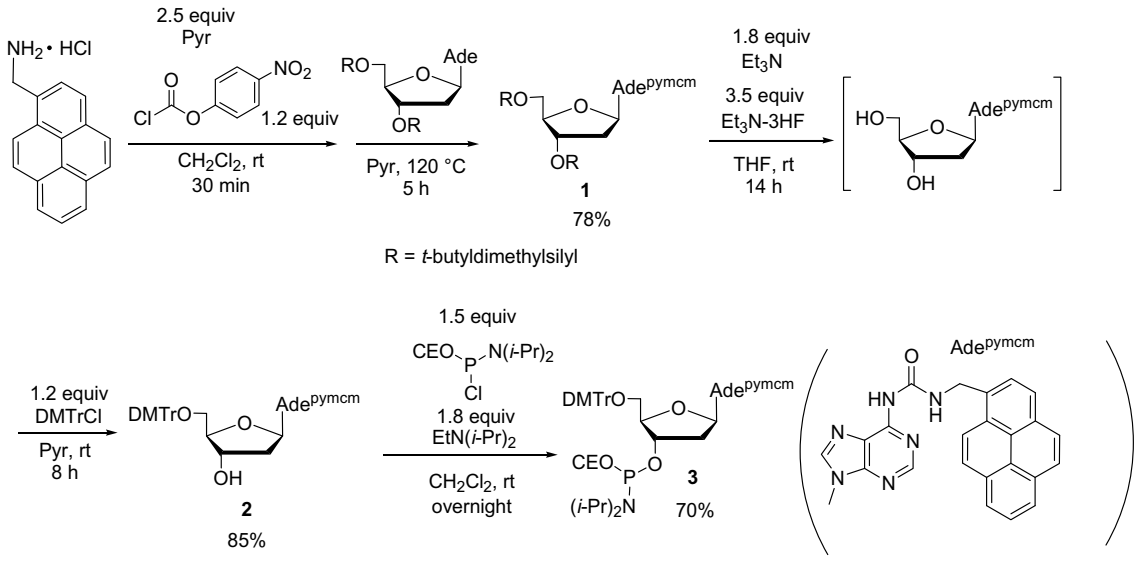

Scheme 1. Synthesis of the pyrene-modified deoxyadenosine derivatives.

of 2.5 equiv of pyridine to give the activated carbamate, which was subsequently condensed with 5 equiv of 2′,3′-*O*-bis(*tert*-butyldimethylsilyl)deoxyadenosine to give desired pyrene-modified silylated deoxyadenosine derivative **1** in 78% yield. The *tert*-butyldimethylsilyl groups were removed by treatment with 3.5 equiv of triethylamine trihydrofluoride in the presence of 1.8 equiv of triethylamine to give a 3′,5′-free derivative, which in turn was treated with 1.2 equiv of DMTrCl to give the protected nucleoside **2** in 85% yield. Finally, the 3′-hydroxyl group was phosphitylated according to the usual procedure to give the phosphoramidite **3**.

Using phosphoramidite **3**, ODNs incorporating dA^{pymcm} were synthesized. The nucleotide sequences of the synthesized ODNs are listed in Scheme 2. **ODN1** and **ODN2** are the oligodeoxynucleotides incorporating a dA^{pymcm} residue and two consecutive dA^{pymcm} residues in the middle of the strand, respectively. **ODN3** incorporates two consecutive dA^{pymcm} residues in the site close to the 5′-terminus of the strand. The **target-DNA** and **target-RNA** which are the oligonucleotides used in the hybridization experiments with **ODN1**, **ODN2**, and **ODN3** are also shown in Scheme 2.

ODN1: d(TTTCTC[A^{pymcm}]TTCTCT)
ODN2: d(TTCTCTTTTCT[A^{pymcm}][A^{pymcm}]TTCTCTTTCTCT)
ODN3:d(CTC[A^{pymcm}][A^{pymcm}]TATACAACCT)

Counter strands for **ODN1**

Target-DNA-1a: d(AGAGAATGAGAAA)
1b: d(AGAGAAAGAGAAA)
1c: d(AGAGAAGGAGAAA)
1d: d(AGAGAACGAGAAA)

Counter strands for **ODN2**

Target-DNA-2a: d(AGAGAAAGAGAATGAGAAAAGAGAA)
2b: d(AGAGAAAGAGAAAGAGAAAAGAGAA)
2c: d(AGAGAAAGAGAAGGAGAAAAGAGAA)
2d: d(AGAGAAAGAGAACGAGAAAAGAGAA)

Target-RNA-2a: r(AGAGAAAGAGAAUGAGAAAAGAGAA)
2b: r(AGAGAAAGAGAAAGAGAAAAGAGAA)
2c: r(AGAGAAAGAGAAGGAGAAAAGAGAA)
2d: r(AGAGAAAGAGAACGAGAAAAGAGAA)

Counter strands for **ODN3**

Short DNA: 5'-d(AGGTTGTATA)-3'
Long DNA: 5'-d(AGGTTGTATAGGGAG)-3'

Short RNA: 5'-r(AGGUUGUAUA)-3'
Long RNA: 5'-d(AGGUUGUAUAGGGAG)-3'

Scheme 2. Sequences of ODNs incorporating dA^{pymcm} and the hybridization targets.

First, the hybridization property of **ODN1**, 5′-d(TTTCTC**dA^{pymcm}**TTCTCT)-3′, was studied using the **target-ODN**s, 3′-d(AAAG AG**X**AAGAGA)-5′, where **X** = T (**1a**), A (**1b**), G (**1c**), or C (**1d**) as shown in Scheme 2. The UV-melting experiments revealed the melting temperatures (T_m) of 40 °C for X = T (**target-ODN-1a**), 38 °C for X = A (-**1b**) 40 °C for X = G (-**1c**), and 38 °C for X = C (-**1d**). These nearly equal T_m values for all the four nucleobases at the X position indicated that dA^{pymcm} does not form the base pair with thymidine and does not discriminate any nucleobase at the base-pairing position in the opposite strand like the universal bases because the N1 position of the adenine base was blocked from the base pairing by the intramolecular hydrogen bond with the NH group of the carbamoyl group as shown in Figure 1.[15,16]

2.2. Fluorescent properties of ODN1 in single and double strand states

Next, we studied the fluorescence properties of **ODN1** in the single- and the double-stranded states formed with the four counter strands, **target-DNA-1a**, **1b**, **1c**, and **1d**. As shown in Figure 2, the fluorescence intensity was weakest in its single-stranded state. When the target strands were added, the intensities increased depending on the opposite base (X) in the order of X = A (**target-DNA-1b**) > T (-**1a**) > G (-**1c**) > C (-**1d**). It is well known that pyrene derivatives become more emissive in aqueous media than in non-aqueous media.[1–5,14] Therefore, larger fluorescence intensities of the double strands compared to the single strand indicated that the pyrene residue exposed in the surrounding aqueous media in the duplex state than in the single strand state. It was also observed that the fluorescence intensity of pyrene was quenched by interaction with the nucleobases at position X, and the quenching was most significant in the interaction with cytosine and least significant with adenine. Therefore, the fluorescence intensities could be partly explained by the interaction with the base opposite to dA^{pymcm}. The small fluorescence intensities of the G-counter strand

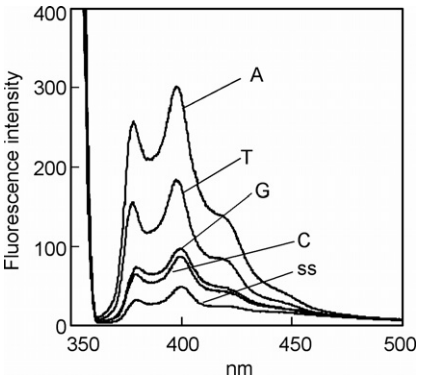

Figure 2. Fluorescence spectra of **ODN1** (2.0 μM) in the absence (ss) or the presence of the**target-DNA**, 5′-d(AGAGAAXGAGAAA)-3′ where X = T (**target-DNA-1a**), A (-**1b**), G (-**1c**), or C (-**1d**) measured at 20 °C.

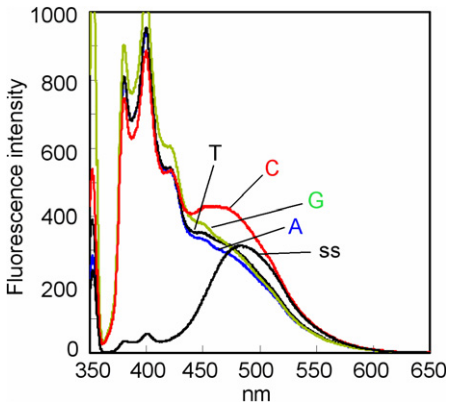

Figure 3. Fluorescence spectra of **ODN2** (1.0 μM) in the presence or the absence (ss) of the 5′-d(AGA GAA AGA GAA **X**GA GAA AAG AGA A)-3′ (X = A, T, G, or C) measured at 20 °C.

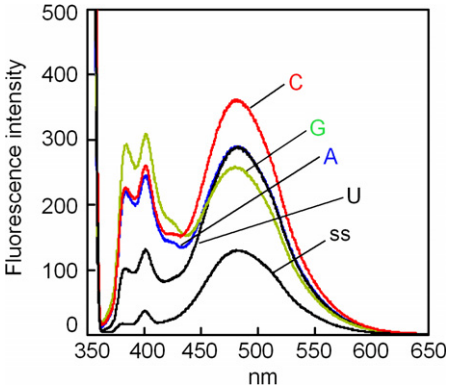

Figure 4. Fluorescence spectra of **ODN2** (0.4 μM) measured at 20 °C in the presence or the absence of the RNA targets 5′-r(AGA GAA AGA GAA XGA GAA AAG AGA A)-5′ (X = A, U, G or C).

is probably due to the charge transfer from the guanine to pyrene producing the guanine radical cation. The C- and T-counter strands probably promote an electron transfer from the pyrene to the C or T producing the cytosine and thymine radical anion as indicated by the previous report on the dependence of the pyrene fluorescence on the redox behavior of the DNA bases.[17]

2.3. Fluorescent properties of ODN2 in the single and double strand state

Next, we examined the fluorescence properties of **ODN2** having two consecutive dA^{pymcm} residues. We expected excimer formation depending on the hybridization. In these experiments, the DNA sequences **target-DNA-2a**, **2b**, **2c**, **2d**, 5′-d(AGAGAAAGAGAA**X**GAG AAAAGAGAA)-3′, where X = A (-**2a**), T (-**2b**), G (-**2c**), or C (-**2d**), were used as the targets. In these sequences, the nucleotide residue positioned at the opposite site to the second dA^{pymcm} residue of the 5′-dA^{pymcm}dA^{pymcm}-3′ dimer was arbitrarily fixed to guanine as indicated by the underline in the sequence, because no base discrimination was observed for dA^{pymcm} residue as indicated by the T_m analyses. In the single-stranded state, the fluorescence spectrum of **ODN2** showed a peak at around 490 nm, which corresponded to the excimer of the two pyrenes. Very small peaks corresponding to those of the monomer were also detected at around 400 nm. Interestingly, upon addition of the target strands, the intensity of the monomer peaks increased. These results can be explained as follows. In the flexible single-stranded state, the two dA^{pymcm} residues could change the conformation rather freely. Therefore, the two hydrophobic pyrene rings could stack on each other to avoid the contact with the aqueous media, thus giving the excimer peak. When the duplexes were formed, one of the dA^{pymcm} residues or both the dA^{pymcm} residues intercalated in the duplex, and the interaction between the two pyrene residues was released. As a result, the dA^{pymcm}dA^{pymcm} site can serve as an indicator of hybridization by measuring the fluorescence intensity at around 400 nm.

We also examined the hybridization-dependent fluorescences of **ODN2** by changing the hybridization target to the RNAs such as **Target-RNA-2a** to **2d**: 5′-r(AGA GAA AGA GAA **X**GA GAA AAG AGA A)-3′, where X = U (-**2a**), A (-**2b**), G (-**2c**), or C (-**2d**). The results are shown in Figure 4. In contrast to the case of the **ODN2**–DNA duplexes, the addition of the target RNA strands leads to an increase in both the monomer and the excimer peaks although increase ratio of the monomer peaks and the excimer peaks differed depending on the nucleobase at position X. This simultaneous increase of both monomer and the excimer peaks was in clear opposition to that shown in Figure 3, wherein the monomer peak increased on addition of the target DNAs.

The presence of both the excimer peaks and the monomer peaks of the **ODN2**–RNA duplexes indicated that the two pyrene residues are in the equilibrium between the monomers and a stacked dimer. This result suggested that the intercalation of the pyrene into the duplexes became less favorable because the A-type **ODN2**–RNA duplexes were more rigid than the B-type conformation of the **ODN2**–DNA duplexes. Similar, DNA–DNA duplex selective intercalation of the pyrene moiety introduced to the 2′-position of probe ODN was also reported.[4]

2.4. Fluorescent properties of ODN3 in the hybridization with DNA and RNA targets having different size

Next, we examined the fluorescent properties of 15mer **ODN3**: d(CTC[A^{pymcm}][A^{pymcm}]TATACAACCT) which incorporate the two consecutive dA^{pymcm} residues at the positions close to the 5′-terminus. The experiments were designed as described below. The 15mer **ODN3** having the dA^{pymcm}dA^{pymcm} near the 5′-terminus was synthesized. As the hybridization targets, the 10mer **short-DNA**: 5′-d(AGGTTGTATA)-3′ which is complementary to the 5′-TATACAACCT-3′ part of **ODN3** and the 15mer **long-DNA**: 5′-d(AGGTTGTATAGGGAG)-3′ which included the additional five nucleotides at the 3′-termini of **short-DNA**. Each of the **short-DNA** and **long-RNA** was added to a solution containing **ODN3**, and the fluorescence properties of the dA^{pymcm}dA^{pymcm} part were monitored. In the single strand state, **ODN3** gave both the monomer's and excimer's peaks at around 400 nm and 490 nm,

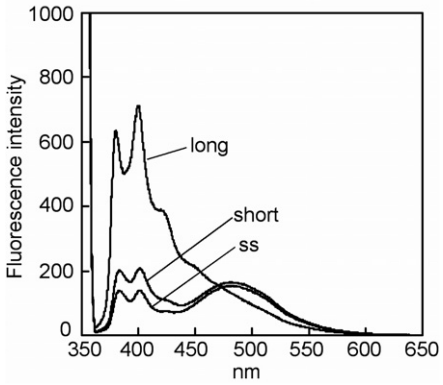

Figure 5. Fluorescence spectra of **ODN3** (0.7 μM) measured at 10 °C in the presence or the absence of the target DNA. short, **ODN3** + 10mer **short-DNA**; long, **ODN3** + 15mer **long-DNA**; ss, **ODN3**.

respectively, as shown in Figure 5. The relative intensities of the monomer's peak and the excimer's peak of the single-stranded **ODN3** were somewhat different from that of **ODN2** in which the $dA^{pymcm}dA^{pymcm}$ dimer was introduced at the central position of the strand. This result suggests that the two pyrene residues in **ODN2** were more tightly fixed in the stacked conformation than in **ODN3** probably because the $dA^{pymcm}dA^{pymcm}$ dimer can move more freely near the 5′ terminal site than in the central position.

As shown in Figure 5, the fluorescence spectrum in the presence of **short-DNA** showed both the excimer peak and the monomer peaks as in the case of the single-stranded **ODN3**. On the other hand, the excimer peak disappeared and the monomer peaks became significantly larger in the duplex with the **long-DNA**.

The results showed that **ODN3** could discriminate the target DNA which was shorter than itself from the longer target at the 5′-terminal region. This size-dependent fluorescence could be explained as follows. In the duplex with the 10mer **short-DNA** target, the $dA^{pymcm}dA^{pymcm}$ site existed as the single strand because $dA^{pymcm}dA^{pymcm}$ was located at the 11th and 12th positions from the 3′-terminus. In this case, the excimer peak was observed, as described in Figure 3. In contrast, the $dA^{pymcm}dA^{pymcm}$ site was present as the duplex to give the monomer peak when **ODN3** was bound to the 15mer **long-DNA** target. These results clearly showed an interesting property of **ODN3** that it changed its fluorescence when the 5′-terminal region dangled. Similar increase of the monomer's peak of the bis-pyrene-modified oligodeoxynucleotides upon binding to the longer DNA was already reported by Yamana et al.[8]

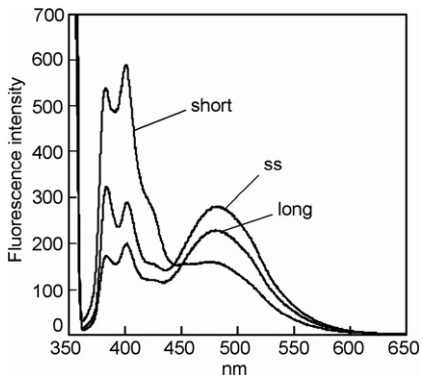

Figure 6. Fluorescence spectra of **ODN3** (1.0 μM) measured at 10 °C in the presence or the absence of the target RNA. short, **ODN3** + **short-RNA**; long, **ODN3** + **long-RNA**; ss, **ODN3**.

The size-dependent fluorescence of **ODN3** would be more useful if it could discriminate the RNA targets rather than DNA targets. In living cells, many small functional RNAs need to be processed from the long precursor RNAs transcribed from the genome. The processing of the miRNA from the pre-miRNA is a good example.[18–20] In the analyses of such functional RNAs, both the sequence and the size of the RNAs must be important in distinguishing the already processed functional miRNA from the non-functional pre-miRNAs.[21] Therefore, we studied the fluorescence of **ODN3** when hybridized to the 10mer **short-RNA**: 3′-AUAUGUUGGA-5′, and the 15mer t**long-RNA:** 3′-GAGGGAUAUGUUGGA-5′. The results are shown in Figure 6.

In this case, the target dependence of the fluorescence of **ODN3** was quite different from that observed using the DNA target shown in Figure 5. In the single-stranded state, **ODN3** gave the fluorescence of the excimer as already shown in Figure 5. In the presence of the **long-RNA** target both the monomer and the excimer peaks were observed similarly. In contrast, in the presence of the **short-RNA** target, the emission of the excimer decreased while that of the monomer increased. These results suggested the ratio of the monomer peak at around 400 nm, and the excimer peak at 490 nm of **ODN3** can be used as an indicator of the chain length of the RNA targets at their 3′-terminal region.

The unique fluorescence properties of **ODN3** in the presence of the RNA targets could not simply be explained from the results shown in Figure 4. The presence of both the excimer and monomer peaks in the case of **ODN3** + **long-RNA** is similar to the case of the hybridization-dependent fluorescence of **ODN2** and RNA targets shown in Figure 4. However, while the fluorescence intensities of **ODN2** were higher in the presence of the targets strands than in the single strand state, those of **ODN3** + **long-RNA** were smaller than those in the single strand state of **ODN3**. Moreover, the increase in the monomer peaks and the decrease of the excimer peak in the duplex with the **short-RNA** target could not be expected at all from Figure 4. The increase of the monomer peak and the decrease of the excimer peak indicated that at lease one of the pyrene residues could intercalate to the nearby base pair so that the stacked pyrene dimer was dissociated to produce the monomer emission especially when the nearby base pair was rather fragile terminal base pair. Although more detailed structural studies are required, the results observed here showed that the conformation of the $dA^{pymcm}dA^{pymcm}$ site of **ODN3** was very sensitive to the structure of the nearby sites so that the fluorescence properties of this site became sensitive to the chain length of the RNA targets at their 3′-terminal region.

2.5. CD and UV spectra of duplexes containing ODN3

In order to obtain the structure property of the duplexes of **ODN3** and the targets we measured the CD spectra of **ODN3** + **short-DNA** and **ODN3** + **long-DNA** (Fig. 7). As shown in Figure 7, the duplex with **short-DNA** gave the spectrum of a standard B-type duplex giving a positive peak at 280 nm and a negative peak at 240 nm. In addition a small peak which could be assigned to that of the pyrene residues was observed at around 370 nm. Interestingly, when **ODN3** formed a duplex with the **long-DNA**, the positive peak and the negative peak shifted to shorter wave lengths and a new positive peak appeared at 290 nm. In addition, the signal from the pyrene residues increased and shifted to a shorter wave length slightly. These observations suggested that the B-type structure was distorted by the steric hindrance of the pyrenylmethyl group when **ODN3** bound to **long-DNA**.

We also measured the CD spectra of **ODN3** + **short-RNA** and **ODN3** + **long-RNA** (Fig. 8). In these cases, both spectra showed that the A-type duplexes gave a positive peak at 270 nm and a negative peak at 210 nm. The pyrene residues gave only small peaks at

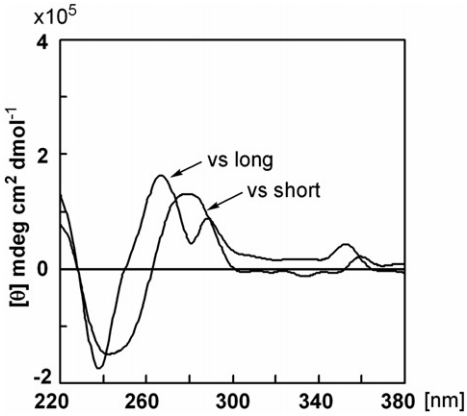

Figure 7. Fluorescence spectra of **ODN3** (2.0 μM) measured at 10 °C in the presence of the target DNA. short, **ODN3** + **short-DNA**; long, **ODN3** + **long-DNA**.

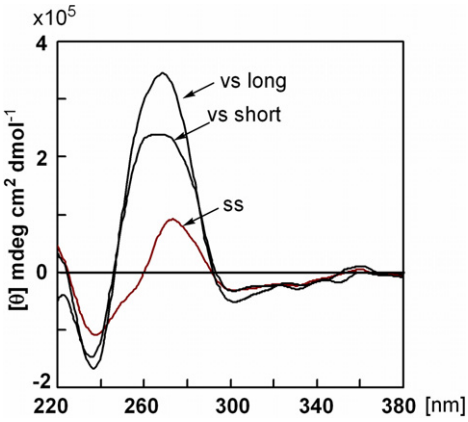

Figure 8. Fluorescence spectra of **ODN3** (2.0 μM) measured at 10 °C in the presence or the absence of the target RNA. ss, **ODN3**; short, **ODN3** + **short-RNA**; long, **ODN3** + **long-RNA**.

370 nm which suggested less effective interaction between the pyrene residues and the nucleobases.

It is well known that the stacking between the nucleobases and the pyrene residue could be monitored by the UV absorption maxima of the pyrene residue. When the UV spectra of **ODN3** + **long-DNA** and **ODN3** + **short-DNA** are compared, the peak at 350 nm was lower and broader in the case of the duplex with **short-DNA**, but the peak positions were almost identical showing only

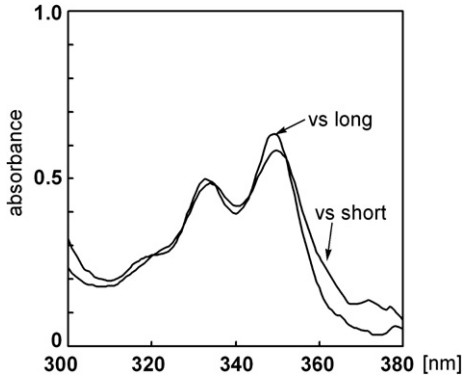

Figure 9. UV spectra of **ODN3** (2.0 μM) measured at 10 °C in the presence of the target DNA. short, **ODN3** + **short-DNA**; long, **ODN3** + **long-DNA**.

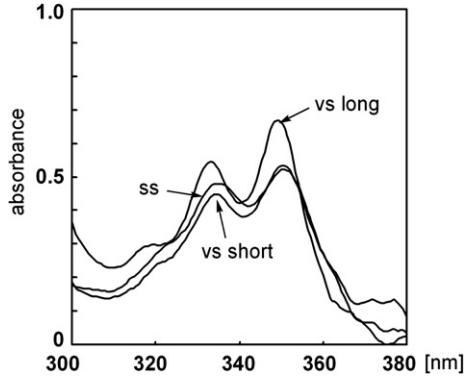

Figure 10. UV spectra of **ODN3** (2.0 μM) measured at 10 °C in the presence of the target DNA. ss, **ODN3**; short, **ODN3** + **short-RNA**; long, **ODN3** + **long-RNA**.

slight blue-shift (ca. 1 nm) in these two duplexes (Fig. 9). Therefore, the interactions between the pyrene residues and the nucleobases did not seem to be the π–π stack interaction. In the case of the duplexes with the RNA targets (Fig. 10), the spectra of **ODN3** + **long-RNA** were almost identical to that of **ODN3** + **long-DNA** at the 300–380 nm region despite a difference in the fluorescent spectra between them. Similarly to the case of **ODN3** + **short-DNA**, the peak hight at 350 nm was lowered and broadened in the case of **ODN3** + **short-RNA**.

3. Conclusion

In this study, we report oligonucleotides incorporating dA^{pymcm}. The **ODN1** singly modified by dA^{pymcm} showed hybridization-dependent fluorescence increase depending on the nucleobases positioned at the opposite site of dA^{pymcm}. When two dA^{pymcm} residues were incorporated consecutively in the middle of ODN such as **ODN2**, the ODN showed hybridization induced increase of the fluorescence depending on the targets strand. **ODN2** gave the pyrene excimer's fluorescence peak in its single strand state. When it bound to the target DNAs, as a rule-of-thumb, the excimer's peak reduced and pyrene monomer's peak increased. When it bound to the target RNAs both the excimer's and monomer's peak were observed.

In this study, we also designed **ODN3** which incorporated two consecutive dA^{pymcm} residues to demonstrate the size discrimination of the target strands by hybridization. The behavior of **ODN3** when it bound to the 10mer and 15mer DNA targets was the one expected from the behavior of **ODN2** and another bis-pyrenyl-modified ODNs reported previously.[8] Therefore, such fluorescence properties might be common to modified oligonucleotides having two pyrene groups at nearby positions. In contrast, the behavior when it bound to 10mer and 15mer RNAs are more complicated but interesting. The **ODN3** gave both excimer's and monomer's fluorescence in the single strand state and when bound to the 15mer RNA. In contrast, it gave mainly the monomer's peak when bound to the shorter RNA. We could not explain at this time this behavior of **ODN3** on the basis of detailed structure of the duplexes of **ODN3** and the RNA targets. The prediction of the duplex structures including dA^{pymcm} dimer does not seem simple. Because the adenine part and the pyrene part are not in a plane in the energy minimized structure due to the presence of a sp3 hybridized carbon atom between the pyrene ring and the carbamoyl group (Fig. 11), the intercalation of the pyrene ring is likely accompanied by some conformation changes of the strands and the nucleoside backbones. Such conformation changes must be analyzed by use of 2D NMR or other techniques in detail and are not clarified yet.

However, the behaviors of **ODN3** are very interesting and might be useful for the design of new oligonucleotide probes

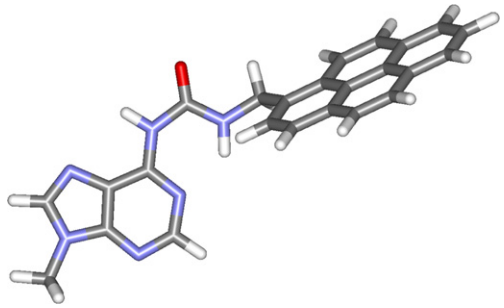

Figure 11. The energy minimized structure of 9-*N*-methyl-N^6-(*N*-pyrenylmethylcarbamoyl)adenine calculated at the HF/6-31G** level by use of GAUSSIAN03 program.[22]

which can recognize both the sequence and the size of RNA targets. Such probes seem useful for the detection of the functional RNAs such as miRNAs, which are transcribed from genome DNAs and work after being processed to short RNA fragments. Currently, the differences in the fluorescence intensity between **ODN3**/**long-RNA** duplexes and **ODN3**/**short RNA** duplexes were not sufficient in terms of the sensitivity to achieve the discrimination of matured miRNAs and pre-miRNAs in living cells. In addition, the dependence of the fluorescences on the probe and target sequences must be also clarified to be applied to the large scale RNA detection. However, the dynamic properties of the pyrene residues found in this study in combination with more sensitive fluorescent dyes might be useful for the development of more sensitive fluorescent probes capable of the target size discrimination. Further studies are being conducted on the improved design of new oligonucleotide probes based on the results of this study and will be reported later.

4. Experimental

4.1. 3′,5′-*O*-Bis(*tert*-butyldimethylsilyl)-N^6-[*N*-(pyren-1-ylmethyl)carbamoyl]-deoxyadenosine (1)

To the suspension of (pyren-1-ylmethyl)amine (2.7 g, 10.0 mmol) in CH_2Cl_2 (100 mL) were added pyridine (2.0 mL, 25 mmol) and 4-nitrophenyl chloroformate (2.4 g, 12 mmol). The resulting mixture was stirred at ambient temperature for 1 h, and the reaction was quenched by the addition of water (3 mL). The solution was washed twice with saturated aqueous $NaHCO_3$ (100 mL each) and the organic layer was dried over Na_2SO_4, filtered, and evaporated under reduced pressure. To the residue were added dry pyridine (50 mL) and 3′,5′-*O*-bis (*tert*-butyldimethylsilyl)-deoxyadenosine (13.7 g, 30.0 mmol), and the mixture was stirred at 120 °C for 2 h. After the solution was cooled to the ambient temperature, it was diluted with ethyl acetate (100 mL). The solution was washed five times with saturated aqueous $NaHCO_3$ (100 mL each), dried over Na_2SO_4, filtered, and evaporated under reduced pressure. The residue was chromatographed on a silica gel column with hexane/ethyl acetate (3:2, v/v) to give **1** (5.7 g, 78%). ^{1}H NMR ($CDCl_3$, 500 MHz) δ 0.06–0.08 (12H, m), 0.89 (18H, m), 2.40–2.44 (1H, m), 2.56–2.61 (1H, m), 3.74 (1H, dd, J = 11.0, 2.4 Hz), 3.84 (1H, dd, J = 11.0, 3.9 Hz), 4.00 (1H, m), 4.58–4.61 (1H, m), 5.36 (2H, m), 6.42 (1H, t, J = 6.4 Hz), 8.00–8.03 (1H, m), 8.06 (2H, s), 8.11–8.12 (2H, m), 8.17–8.21 (4H, m), 8.30 (2H, d, J = 12.4 Hz), 8.41 (1H, d, J = 9.3 Hz), 10.01–10.03 (1H, m); ^{13}C NMR ($CDCl_3$) δ 18.4, 18.8, 26.1, 26.3, 41.6, 42.8, 63.0, 84.8, 88.4, 121.1, 123.3, 125.2, 125.4, 125.7, 126.4, 127.0, 127.7, 127.8, 128.4, 129.3, 131.1, 131.4, 131.7, 132.0, 141.6, 150.3, 150.5, 151.3, 154.2; HRMS calcd for $C_{40}H_{52}N_6O_4Si_2$ ($M+H^+$) 737.3766. Found 737.3630.

4.2. 5′-*O*-(4,4′-Dimethoxytrityl)-N^6-[*N*-(pyren-1-ylmethyl)carbamoyl]-deoxyadenosine (2)

Compound **1** (3.3 g, 4.5 mmol) was dissolved in THF (23 mL). To this solution were added triethylamine trihydrofluoride (2.6 mL, 16 mmol) and triethylamine (1.1 mL, 8.2 mmol). After being stirred at ambient temperature for 14 h, the solvents were removed under reduced pressure. The residue was chromatographed on silica gel column to give the crude material of the nucleoside. The material was rendered anhydrous by the co-evaporation with dry pyridine three times. The residue was dissolved in dry pyridine (45 mL) and 4,4′-dimethoxytritylchloride (1.8 g, 5.4 mmol) was added. After being stirred at ambient temperature for 5 h, the reaction was quenched by adding water (5 mL). The solvents were evaporated under reduced pressure, and the residue was dissolved in ethyl acetate (100 mL). The solution was washed three times with saturated aqueous $NaHCO_3$ (100 mL each), dried over Na_2SO_4, and concentrated under reduced pressure. The residue was chromatographed on a silica gel column with chloroform/methanol (100:1, v/v) containing 0.5% triethylamine to give **2** (3.1 g, 85%). ^{1}H NMR ($CDCl_3$, 500 MHz) δ 2.49–2.54 (1H, m), 2.76–2.83 (2H, m), 3.35–3.42 (2H, m), 3.71 (6H, s), 4.15–4.18 (1H, dd, J = 4.4, 4.2 Hz), 4.66–4.48 (1H, m), 5.34–5.36 (2H, t, J = 5.1 Hz), 6.40–6.43 (1H, m), 6.75–6.77 (4H, m), 7.15–7.18 (1H, t, , J = 7.3 Hz), 7.21–7.24 (2H, m), 7.28 (4H, d, J = 2.2 Hz), 7.37–7.38 (2H, d, J = 7.3 Hz), 8.00–8.03 (1H, t, J = 7.6 Hz), 8.05 (2H, s), 8.10–8.12 (1H, d, J = 8.5 Hz), 8.14–8.20 (4H, m), 8.39–8.40 (1H, d, J = 9.0 Hz), 8.51 (1H, s), 10.10 (1H, m); ^{13}C NMR ($CDCl_3$) δ 40.2, 42.5, 55.3, 63.7, 72.5, 84.6, 86.2, 86.7, 113.3, 120.9, 123.0, 124.9, 125.0, 125.1, 125.4, 125.4, 126.1, 126.7, 127.1, 127.5, 127.5, 128.0, 128.2, 129.0, 130.1, 130.9, 131.1, 131.4, 131.7, 135.7, 135.7, 141.3, 144.6, 150.0, 150.2, 151.1, 154.0, 158.7; HRMS calcd for $C_{44}H_{44}N_6O_6$ ($M+H^+$) 833.3058. Found 833.3093.

4.3. 5′-*O*-(4,4′-Dimethoxytrityl)-N^6-[*N*-(pyren-1-ylmethyl)carbamoyl]deoxyadenosine 3′-(2-cyanoethyl *N*,*N*-diisopropylphosphoramidite) (3)

Compound **2** (320 mg, 0.4 mmol) was rendered anhydrous by co-evaporation twice with dry toluene, twice with dry acetonitrile, and once with dry CH_2Cl_2, and finally dissolved in dry CH_2Cl_2 (4 mL). To this solution were added *N*,*N*-diisopropylethylamine (125 μL, 0.72 mmol) and chloro(2-cyanoethoxy)(*N*,*N*-diisopropylamino)phosphine (140 mg, 0.6 mmol). After being stirred at ambient temperature for 18 h, the reaction was quenched by addition of water (500 μL). The solvents were evaporated under reduced pressure, and the residue was dissolved in ethyl acetate/ethyl ether (3 mL, 1:2, v/v). The solution was washed eight times with 0.2 M NaOH (3 mL, each), dried over Na_2SO_4 and concentrated under reduced pressure. The residue was chromatographed on a gel-filtration column with $CHCl_3$ to give **3** (280 mg, 70%). ^{1}H NMR (DMSO, 500 MHz) δ 1.00–1.13 (12H, m), 2.52–2.59 (1H, m), 2.64–2.66 (2H, m), 3.05–3.12 (1H, m), 3.16–3.29 (2H, m), 3.48–3.59 (2H, m), 3.61–3.78 (2H, m), 3.65–3.66 (6H, m), 4.09–4.16 (1H, m), 4.76–4.82 (1H, m), 5.24–5.27 (2H, m), 6.42–6.46 (1H, m), 6.71–6.77 (4H, m), 7.08–7.28 (9H, m), 8.07 (1H, t, J = 7.56 Hz), 8.13–8.17 (3H, m), 8.28–8.33 (H, m), 8.50 (1H, d, J = 9.27 Hz), 8.54 (1H, d, J = 5.61 Hz), 9.85 (1H, s), 10.0 (1H, t, J = 5.12 Hz); ^{13}C NMR (DMSO) δ 19.7, 19.8, 19.9, 24.1, 24.2, 24.3, 24.4, 41.2, 42.5, 42.6, 54.9, 54.9, 58.3, 58.4, 58.5, 63.3, 63.4, 72.5, 79.2, 84.0, 84.7, 85.0, 85.5, 112.9, 113.0, 118.8, 119.0, 120.6, 123.0, 123.9, 124.1, 124.9, 125.2, 125.3, 126.2, 126.3, 126.5, 127.1, 127.5, 127.6, 127.7, 128.0, 129.5, 129.6, 130.2, 130.3, 130.8, 132.9, 135.3, 135.4,

142.7, 142.8, 144.7, 149.9, 150.3, 150.5, 153.5, 158.0, 158.0; ^{31}PNMR (DMSO) δ 148.1, 148.8. HRMS calcd for $C_{58}H_{59}N_8O_7P$ ($M+H^+$) 1033.4136. Found 1033.4779.

4.4. Oligonucleotide synthesis

The oligonucleotides incorporating dA^{pymcm} residues were synthesized by using phosphoramidite **3** on an automated DNA synthesizer. The cleavage of the synthesized 5′-DMTr-oligonucleotide from the solid support and the deprotection of the nucleobases were carried out by treatment with 28% aqueous ammonia at room temperature for 24 h. The products were purified according to the standard Trityl-ON procedure followed by the purification on an anion-exchange HPLC by use of 0–50% gradient of 1 M NaCl in 25 mM sodium phosphate–10% CH_3CN. The sequences and the results of the mass analyses are shown below.

ODN1: d(TTTCTC[A^{pymcm}]TTCTCT), mass calcd $[M+H]^+$ 4109.3, found 4099.8.

ODN2: d(TTCTCTTTTCT[A^{pymcm}][A^{pymcm}]TTCTCTTTCTCT), mass calcd $[M+H]^+$ 7967.4, found 7974.2.

ODN3: d(CTC[A^{pymcm}][A^{pymcm}]TATACAACCT), mass calcd $[M+H]^+$ 4993.0, found 4993.8.

4.5. T_m measurement

Each oligonucleotide was dissolved in 10 mM sodium phosphate (pH 7.0) containing 100 mM NaCl and 0.1 mM EDTA so that the final concentration of each oligonucleotide became 2 μM. The solution was separated into quartz cells (10 mm) and incubated at 85 °C. After 10 min the solution was cooled to 5 °C at the rate of 0.5 °C/min and heated to 85 °C at the same rate. During this annealing and melting, the absorption at 260 nm was recorded and used to draw UV-melting curves. The T_m value was calculated as the temperature that gave the maximum of the first derivative of the UV-melting curve. The molar extinction constant (ε_{260}) of **ODN1** was estimated to be 107,600 assuming the extinction coefficient are equal to that of 5′-d(TTTCTCATTCTCT)-3′. The molar extinction constants (ε_{260}) of **ODN2** and **ODN3** were determined as 214,000 and 141,000 after the enzymatic digestion according to the general procedure. For example, **ODN3** (0.97 OD_{260}) was dissolved in 290 μL of 10 mM phosphate (1 M NaCl, pH 7.0). To this solution was added nuclease P1 (6 μL, 3 U), phosphodiesterase I from *Crotalus adamanteus* (3 μL, 0.03 mg) and calf intestine alkaline phosphatase (2 μL, 2 U). The solution was incubated at 37 °C for 12 h and then quenched by heating for 1 min at 80 °C. After removing the enzyme by a filtration, the aliquot (50 μL) was analyzed by a reversed-phase HPLC. The peak area was quantified by comparing with those of the 50 μL of the standard sample containing 0.1 mM of deoxyadenosine, deoxyguanosine, deoxycytidine, and thymidine.

4.6. Fluorescence measurement

An ODN incorporating dA^{pymcm} and the target strand was dissolved in 10 mM sodium phosphate buffer (pH 7.0) containing 1.0 M NaCl. Fluorescence spectra were obtained at 10 °C in the absence or the presence of the small excess (1.2 equiv) of the target DNAs and RNAs in a 1 cm path length cell. The oligonucleotide concentrations were adjusted so that the fluorescence signal did not exceeded 1000. The concentrations of the pyrene-modified oligonucleotides were 2.0 μM for the experiments shown in Figure 2, 1.0 μM for Figure 3, 0.4 μM for Figure 4, 0.7 μM for Figure 5, and 1.0 μM for Figure 6.

The melting temperatures of the 2 μM duplexes containing **ODN3** were 37 °C for **ODN3** + **short-RNA**, 44 °C for **ODN3** + **long-RNA**, 47 °C for **ODN3** + **short-DNA**, and 49 °C for **ODN3** + **long-RNA**.

4.7. UV and CD measurement

Each duplex was dissolved in 10 mM sodium phosphate (pH 7.0) containing 100 mM NaCl and 0.1 mM EDTA so that the final concentration of each oligonucleotide became 2 μM. The spectra were measured at 10 °C.

Acknowledgments

This study was supported by Industrial Technology Research Grant Program in '05 from New Energy and Industrial Technology Development Organization (NEDO) of Japan. This work was also financially supported partly by a Grant-in-Aid from CREST, Japan Science and Technology Agency and the Ministry of Education, Science, Sports and Culture, Grant-in-Aid for Scientific Research.

References and notes

1. Kierzek, R.; Li, Y.; Turner, D. H.; Bevilacqua, P. C.. *J. Am. Chem. Soc.* **1993**, *115*, 4985–4992.
2. Bevilacqua, P. C.; Kierzek, R.; Johnson, K. A.; Turner, D. H. *Science* **1992**, *258*, 1355–1358.
3. Mann, J. S.; Shibata, Y.; Meehan, T. *Bioconjugate Chem.* **1992**, *3*, 554–558.
4. Nakamura, M.; Fukunaga, Y.; Sasa, K.; Ohtoshi, Y.; Kanaori, K.; Hayashi, H.; Nakano, H.; Yamana, K. *Nucleic Acids Res.* **2005**, *33*, 5887–5895.
5. Okamoto, A.; Kanatani, K.; Saito, I. *J. Am. Chem. Soc.* **2004**, *126*, 4820–4827.
6. Lewis, F. D.; Zhang, Y.; Letsinger, R. L. *J. Am. Chem. Soc.* **1997**, *119*, 5451–5452.
7. Telser, J.; Cruickshank, K. A.; Morrison, L. E.; Netzel, T. L. *J. Am. Chem. Soc.* **1989**, *111*, 6966–6976.
8. Yamana, K.; Iwai, T.; Ohtani, Y.; Sato, S.; Nakamura, M.; Nakano, H. *Bioconjugate Chem.* **2002**, *13*, 1266–1273.
9. Okamoto, A.; Ichiba, T.; Saito, I. *J. Am. Chem. Soc.* **2004**, *126*, 8364–8365.
10. Kumar, T. S.; Wengel, J.; Hrdlicka, P. J. *ChemBioChem* **2007**, *8*, 1122–1125.
11. Fujimoto, K.; Shimizu, H.; Inouye, M. *J. Org. Chem.* **2004**, *59*, 3271–3275.
12. Paris, P. L.; Langenhan, J. M.; Kool, E. T. *Nucleic Acids Res.* **1998**, *26*, 3789–3793.
13. Christensen, U. B.; Pedersen, E. B. *Nucleic Acids Res.* **2002**, *30*, 4918–4925.
14. Kalyanasundaram, K.; Thomas, J. K. *J. Phys. Chem.* **1977**, *81*, 2176–2180.
15. Miyata, K.; Tamamushi, R.; Ohkubo, A.; Taguchi, H.; Seio, K.; Sekine, M. *Tetrahedron Lett.* **2004**, *45*, 9365–9368.
16. Nakano, S.; Uotani, Y.; Uenishi, K.; Fujii, M.; Sugimito, N. *Nucleic Acids Res.* **2005**, *33*, 7111–7119.
17. Manoharan, M.; Tivel, K. L. *J. Phys. Chem.* **1995**, *99*, 17461–17472.
18. Ambros, V. *Cell* **2001**, *107*, 823–826.
19. Bartel, D. P. *Cell* **2004**, *116*, 281–297.
20. Cullen, B. R. *Mol. Cell* **2004**, *16*, 861–865.
21. Chen, C.; Ridzon, D. A.; Broomer, A. J.; Zhou, Z.; Lee, D. H.; Nguyen, J. T.; Barbisin, M.; Xu, N. L.; Mahuvakar, V. R.; Andersen, M. R.; Lao, K. Q.; Livak, K. J.; Guegler, K. J. *Nucleic Acids Res.* **2005**, *33*, e179.
22. Frisch, M. J.; Trucks, G. W.; Schlegel, H. B.; Scuseria, G. E.; Robb, M. A.; Cheeseman, J. R.; Montgomery, J. A., Jr.; Vreven, T.; Kudin, K. N.; Burant, J. C.; Millam, J. M.; Iyengar, S. S.; Tomasi, J.; Barone, V.; Mennucci, M.; Cossi, M.; Scalmani, G.; Rega, N.; Petersson, G. A.; Nakatsuji, H.; Hada, M.; Ehara, M.; Toyota, K.; Fukuda, R.; Hasegawa, J.; Ishida, M.; Nakajima, T.; Honda, Y.; Kitao, O.; Nakai, H.; Klene, M.; Li, X.; Knox, J. E.; Hratchian, H. P.; Cross, J. B.; Adamo, C.; Jaramillo, J.; Gomperts, R.; Stratmann, R. E.; Yazyev, O.; Austin, A. J.; Cammi, R.; Pomelli, C.; Ochterski, J. W.; Ayala, P. Y.; Morokuma, K.; Voth, G. A.; Salvador, P.; Dannenberg, J. J.; Zakrezwski, V. G.; Dapprich, S.; Daniels, A. D.; Strain, M. C.; Farkas, O.; Malick, D. K.; Rabuck, A. D.; Raghavachari, K.; Foresman, J. B.; Ortiz, J. V.; Cui, Q.; Baboul, A. G.; Clifford, S.; Cioslowski, J.; Stefanov, B. B.; Liu, G.; Liashenko, A.; Piskorz, P.; Komaromi, I.; Martin, R. L.; Fox, D. J.; Keith, T.; Al-Laham, M. A.; Peng, C. Y.; Nanayakkara, A.; Challacombe, M.; Gill, P. M. W.; Johnson, B.; Chen, W.; Wong, M. W.; Gonzalez, C.; Pople, J. A. *Gaussian 03, Revision C.02*; Gaussian, Inc.: Pittsburgh PA, 2003.